Advanced Composite Materials, 2016
http://dx.doi.org/10.1080/09243046.2015.1126665

Taylor & Francis
Taylor & Francis Group

Electric current distribution of carbon fiber reinforced polymer beam: analysis and experimental measurements

Takuya Yamane[a], Akira Todoroki[a]*, Hiroyasu Fujita[b], Ai Kawashima[b] and Naoki Sekine[b]

[a]*Department of Mechanical Sciences and Engineering, Tokyo Institute of Technology, Box I1-58, 2-12-1 Ookayama, Meguro, Tokyo 152-8552, Japan;* [b]*Aerospace Company, Fuji Heavy Industries Ltd., 1-1-11 Yonan, Utsunomiya-shi, Tochigi 320-8564, Japan*

(*Received 23 August 2015; accepted 27 November 2015*)

The authors have previously proposed an effective method for analyzing the electric current density of carbon fiber-reinforced polymer (CFRP) composites using an anisotropic electric potential function. The method is based on the assumption that CFRP laminates are homogeneous orthotropic materials. Actual CFRP laminates are, however, heterogeneous materials, having resin-rich layers and carbon fiber layers. In the present study, the electric conductance is calculated on the assumption that CFRP laminates are homogeneous using electrical resistance data measured by a four-probe method, and used for electric current analysis. A new specimen design is proposed to allow the electric current distribution of CFRP laminates to be investigated experimentally. The results obtained confirm that our analysis method is accurate for determining the electric current density of actual CFRP laminates. Thus, the assumption that CFRP laminates may be considered homogeneous orthotropic materials for electric current analysis is experimentally verified.

Keywords: electric current; analysis; experiment; potential flow; electric conductance

1. Introduction

In recent years, the application of carbon fiber-reinforced polymer (CFRP) composites to aircraft structures has expanded because of their excellent specific mechanical properties. The electric conductance of CFRP, however, is relatively low compared with that of conventional metallic materials, and also shows anisotropy. This strongly anisotropic conductivity of CFRP may result in structural damage when lightning strike occurs. Metal foils or meshes are attached to the surface of CFRP components of in-service aircrafts for lighting protection.[1] It is, however, difficult to prevent leak current because of the impulse current. Many research articles concerning damage to CFRP laminates struck by artificial lightning suggest that evaluation of the electric current distribution in such laminates is indispensable for the assessment of the damage to aircraft structural components caused by lightning strike.[2–5] Toughened CFRP laminates have resin-rich interlaminae to prevent delamination cracking. The existence of such resin-rich interlaminae in aircraft structures, however, makes it difficult to evaluate electric current distribution.[6]

*Corresponding author. Email: atodorok@ginza.mes.titech.ac.jp

Todoroki has previously proposed an analytical method to calculate electric current distribution in laminated CFRP.[7,8] In the analysis method, the electric current distribution in a laminated CFRP is calculated using the anisotropic electric potential function. The analysis method assumes that CFRPs are homogeneous orthotropic materials. The toughened CFRP laminates used for aircraft, however, are not homogeneous with respect to the thickness direction because of their resin-rich layers. In the present study, therefore, the electric current calculated using the analytical method is compared with experimental data to confirm the reliability of the analysis method. Because the previously described analysis method [8] is limited to the analysis of long beam specimens (an infinite length beam), in the present study the analysis is modified to reflect actual specimen configuration (a finite length beam). Beam-type CFRP specimens of two types of stacking sequence were prepared: unidirectional and cross-ply laminated CFRP. Using the measured conductivity of the specimens, the electric current was calculated using the analytical model and compared with the experimental results.

2. Analytical method

2.1. Analytical method: unidirectional CFRP laminates

Let us assume that unidirectional CFRP laminates are homogeneous orthotropic materials electrically. The Cartesian two-dimensional coordinate system is defined with the x-axis as the fiber direction and the z-axis as the thickness direction. Let the electric conductance of each direction be σ_x and σ_z, respectively. The electric current density in the x and z directions (i_x, i_z) can be obtained using the anisotropic electric potential function ϕ as follows [7]:

$$i_x = -\sigma_x \frac{\partial \phi}{\partial x}, \quad i_z = -\sigma_z \frac{\partial \phi}{\partial z} \tag{1}$$

Let us consider the semi-infinite plate model having electric current source and sink points described in Figure 1. When a source is located at $(-a, 0)$ and a sink is located at $(a, 0)$, the electric potential function can be obtained using the input current I as follows (refer to reference [7] for detail):

$$\phi = -\frac{I}{2\pi\sqrt{\sigma_x \sigma_z}} \ln \frac{\dfrac{(x-a)^2}{\sigma_x} + \dfrac{z^2}{\sigma_z}}{\dfrac{(x+a)^2}{\sigma_x} + \dfrac{z^2}{\sigma_z}} \tag{2}$$

In the present study, the potential function is modified for the case that the source and the sink (electrical ground) are not infinitely small points but finite-length lines: the source and the sink have each finite length. In actual beam-type specimens, the electric current source and the sink are not infinitely small points, so this modification makes

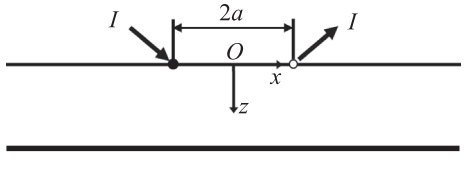

Figure 1. CFRP plate with an electric current input and output points.

the analysis method agree with actual beam type specimens. Figure 2 presents a semi-infinite plate model having a current source and sink of finite length located at distances of t_1 and t_2 from the origin with input current I.

To obtain the electric potential function of the finite length source, the already published electric potential function of the infinitely small source [9] is superposed from t_1 to t_2. The electric potential function of the sink is easily obtained by replacing I with $-I$ of the potential function of source. The potential function ϕ' of the infinitely small source and sink located at distance a from the origin can be expressed by Equation (2) with the replacement of the input current $I/(t_2 - t_1)$ as follows:

$$\phi' = -\frac{I}{2\pi(t_2 - t_1)\sqrt{\sigma_x\sigma_z}} \ln \frac{\frac{(x-a)^2}{\sigma_x} + \frac{z^2}{\sigma_z}}{\frac{(x+a)^2}{\sigma_x} + \frac{z^2}{\sigma_z}} \tag{3}$$

Integrating the potential ϕ' from t_1 to t_2 with respect to a gives the potential function ϕ of the finite-length current source and sink in Figure 2 as follows:

$$\begin{aligned}\phi &= \int_{t_1}^{t_2} \phi' da \\ &= -\frac{I}{2\pi(t_2 - t_1)\sqrt{\sigma_x\sigma_z}} \left[(x + t_2) \ln \left\{ (x + t_2)^2 + \frac{\sigma_x}{\sigma_z} z^2 \right\} - (x + t_1) \ln \left\{ (x + t_1)^2 + \frac{\sigma_x}{\sigma_z} z^2 \right\} \right. \\ &\quad + (x - t_2) \ln \left\{ (x - t_2)^2 + \frac{\sigma_x}{\sigma_z} z^2 \right\} - (x - t_1) \ln \left\{ (x - t_1)^2 + \frac{\sigma_x}{\sigma_z} z^2 \right\} \\ &\quad \left. + 2\sqrt{\frac{\sigma_x}{\sigma_z} z^2} \left(\arctan \frac{x + t_2}{\sqrt{\frac{\sigma_x}{\sigma_z} z^2}} - \arctan \frac{x + t_1}{\sqrt{\frac{\sigma_x}{\sigma_z} z^2}} + \arctan \frac{x - t_2}{\sqrt{\frac{\sigma_x}{\sigma_z} z^2}} - \arctan \frac{x - t_1}{\sqrt{\frac{\sigma_x}{\sigma_z} z^2}} \right) \right]\end{aligned} \tag{4}$$

The electric potential difference function in each axis can be obtained by partial differentiation with respect to each axis as follows:

$$\frac{\partial \phi}{\partial x} = -\frac{I}{2\pi\sqrt{\sigma_x\sigma_z}(t_2 - t_1)} \times \ln \frac{\left\{ (t_2 + x)^2 + \frac{\sigma_x}{\sigma_z} z^2 \right\} \left\{ (t_2 - x)^2 + \frac{\sigma_x}{\sigma_z} z^2 \right\}}{\left\{ (t_1 + x)^2 + \frac{\sigma_x}{\sigma_z} z^2 \right\} \left\{ (t_1 - x)^2 + \frac{\sigma_x}{\sigma_z} z^2 \right\}} \tag{5}$$

$$\begin{aligned}\frac{\partial \phi}{\partial z} &= -\mathrm{sgn}(z) \frac{I}{\pi(t_2 - t_1)\sigma_z} \\ &\quad \times \left(\arctan \frac{x + t_2}{\sqrt{\frac{\sigma_x}{\sigma_z} z^2}} - \arctan \frac{x + t_1}{\sqrt{\frac{\sigma_x}{\sigma_z} z^2}} + \arctan \frac{x - t_2}{\sqrt{\frac{\sigma_x}{\sigma_z} z^2}} - \arctan \frac{x - t_1}{\sqrt{\frac{\sigma_x}{\sigma_z} z^2}} \right)\end{aligned} \tag{6}$$

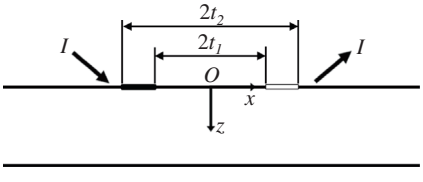

Figure 2. CFRP plate with an electric current input and output lines.

Substituting these functions into Equation (1) gives the analytical solution of the current density. In Figure 2, the electric current density in the x-direction i_x at the center of the model ($x = 0$) can be expressed as follows:

$$i_x = \frac{I}{\pi(t_2 - t_1)}\sqrt{\frac{\sigma_x}{\sigma_z}}\ln\frac{t_2^2 + \frac{\sigma_x}{\sigma_z}z^2}{t_1^2 + \frac{\sigma_x}{\sigma_z}z^2} \tag{7}$$

For the finite plate, the analysis of the infinite plate is not appropriate. To obtain the exact analysis, mirror images of the pairs of sources and sinks have already been used and are proven to be effective for calculation of an exact electric current density.[8,10] Similarly, when the finite plate has a finite-length source and sink as shown in Figure 3, multiple pairs of finite-length sources and sinks must be considered as illustrated in Figure 4. The appropriate number of the sets of images N can be evaluated considering the permeability of electric current compared with the input current I. The fraction of permeated current divided by the input current I is defined as δ_t as follows:

$$\begin{aligned}\delta_t &= \frac{1}{I}\int_{-2NT}^{2NT} i_x dz \\ &= \frac{1}{(t_2 - t_1)\pi}\left\{\sqrt{\frac{\sigma_x}{\sigma_z}}NT\ln\frac{(NT)^2 + \frac{\sigma_z}{\sigma_x}t_2^2}{(NT)^2 + \frac{\sigma_z}{\sigma_x}t_1^2} + 2\left(t_2\arctan\frac{NT}{t_2\sqrt{\frac{\sigma_z}{\sigma_x}}} - t_1\arctan\frac{NT}{t_1\sqrt{\frac{\sigma_z}{\sigma_x}}}\right)\right\}\end{aligned} \tag{8}$$

Assuming that 99% of the input current I flows in the actual finite plate:

$$0.99 \le \frac{1}{(t_2 - t_1)\pi}\left\{\sqrt{\frac{\sigma_x}{\sigma_z}}NT\ln\frac{(NT)^2 + \frac{\sigma_z}{\sigma_x}t_2^2}{(NT)^2 + \frac{\sigma_z}{\sigma_x}t_1^2} + 2\left(t_2\arctan\frac{NT}{t_2\sqrt{\frac{\sigma_z}{\sigma_x}}} - t_1\arctan\frac{NT}{t_1\sqrt{\frac{\sigma_z}{\sigma_x}}}\right)\right\} \tag{9}$$

The required number of image N can be obtained by Equation (9). Summing up the current densities from the image of #–N to that of #N gives us the almost exact analytical results in the finite plate. Using Equations (5) and (7), the electric potential difference function and current density in the x-direction in the finite plate at $x = 0$ can be represented as follows:

$$\frac{\partial\phi}{\partial x} = -\sum_{n=-N}^{n=N}\frac{I}{\pi\sqrt{\sigma_x\sigma_z}(t_2 - t_1)}\ln\frac{t_2^2 + \frac{\sigma_x}{\sigma_z}(z - 2nT)^2}{t_1^2 + \frac{\sigma_x}{\sigma_z}(z - 2nT)^2} \tag{10}$$

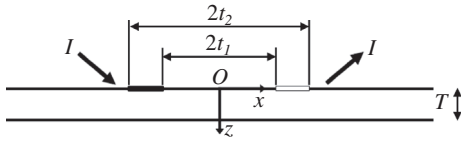

Figure 3. Finite CFRP plate with an electric current input and output lines.

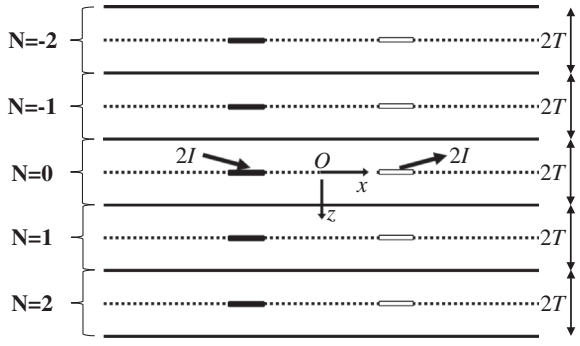

Figure 4. Schematic representation of mirror images method for electric current of a finite CFRP plate.

$$i_x = \frac{I}{\pi(t_2 - t_1)} \sqrt{\frac{\sigma_x}{\sigma_z}} \sum_{n=-N}^{n=N} \ln \frac{t_2^2 + \frac{\sigma_x}{\sigma_z}(z - 2nT)^2}{t_1^2 + \frac{\sigma_x}{\sigma_z}(z - 2nT)^2} \tag{11}$$

2.2. *Equivalent electric conductivity of cross-ply CFRP laminates*

Our previous paper [7] shows that electric current density in orthotropic thick laminates with many 0°-plies can be analyzed using the electric potential distribution of unidirectional thick CFRP of 0°-plies. In the case of a thin plate, however, the electric potential distribution of a unidirectional CFRP is different from that of cross-ply laminates. This means that the equivalent electric conductance that gives the equivalent electric potential distribution in thin cross-ply laminates is required. The method used to calculate this has been described in a previous paper [8] and is shown briefly here.

The equivalent electric conductivity in the x-direction of the cross-ply CFRP laminates is lower than that of the unidirectional CFRP laminates. The decrease in the equivalent conductivity is caused by the low conductivity in the 90°-plies, not only by the fiber direction, but also by the distance from the top surface where the current source and sink affects the electric potential difference. A larger distance causes smaller electric potential difference. The effect of 90°-ply, therefore, must be considered with respect to the distance from the top surface.[11]

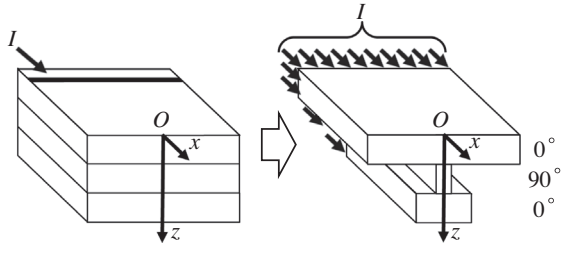

Figure 5. Schematic representation of cross section of CFRP plate, which shows a concept of equivalent electric conductance.

Figure 5 shows a schematic representation of the equivalent cross-sectional area at the center ($x = 0$) of the model in Figure 3. In the equivalent conductivity model, the electric current of the cross-ply laminate in each ply at $x = 0$ (as shown in Figure 5 left) can be replaced by the electric current density of the CFRP that has uneven cross-sectional area, as shown in Figure 5 right.

Figure 5 (right) illustrates the equivalent conductivity model. The reduction in the width of the ply represents the effect of the decreased electric potential difference and small electric conductivity of 90°-ply. In the equivalent model, the uniform electric potential difference is considered to be charged in the uneven cross-section. Using this model, the equivalent conductivity that gives equivalent electric potential difference distribution can be calculated. For cross-ply laminate, the equivalent electric conductance $\overline{\sigma_x}$ is defined as follows:

$$\overline{\sigma_x} = \frac{\sum_{k=1}^{M} \sigma_x(z_k) \frac{\partial \phi(z_k)}{\partial x}}{\sum_{k=1}^{M} \frac{\partial \phi(z_k)}{\partial x}} \tag{12}$$

where M is the number of grids in the thickness direction that are used to calculate the equivalent electric conductance, z_k is the depth from the surface, $\sigma_x(z_k)$ is the electric conductance in the x-direction at a depth of $z = z_k$, and $\partial\phi(z_k)/\partial x$ is the value of the electric potential difference in the x-direction at $z = z_k$. The number of grids M should be larger than the number of plies. The equivalent electric conductance $\overline{\sigma_x}$ can be calculated through the following processes.

(1) Substituting the electric conductivity in the fiber direction and in the thickness direction to σ_x and σ_z, respectively, the electric potential difference function in the x-direction $\partial\phi/\partial x$ is calculated using Equation (10) by assuming the laminate is unidirectional CFRP of 0°-plies.
(2) Using the obtained $\partial\phi/\partial x$ and Equation (12), the equivalent electric conductance $\overline{\sigma_x}$ is calculated.
(3) Substituting the obtained equivalent electric conductance $\overline{\sigma_x}$ and electric conductance in the thickness direction to σ_x and σ_z, respectively, the electric potential difference function in the x-direction $\partial\phi/\partial x$ is newly calculated using Equation (10) by assuming the laminate is a unidirectional CFRP of 0°-plies having different conductivity.
(4) Using the obtained $\partial\phi/\partial x$ and Equation (12), the equivalent electric conductance $\overline{\sigma_x}$ is calculated.
(5) Iterating the process from (3) to (4) until the difference between the obtained $\overline{\sigma_x}$ and previously calculated value is smaller than a threshold of 1.0×10^{-4}.

Using the obtained $\overline{\sigma_x}$, the electric potential difference function in the x-direction is calculated. The electric current distribution can be analyzed using this function and Equation (1). In the calculation of the electric current density, the actual electric conductance in the x-direction at each ply must be used in Equation (1).

2.3. *Measurement of electric conductivity in each direction*

In the present study, two types of stacking sequences of beam-type laminates were prepared: unidirectional CFRP $[0]_8$ and cross-ply CFRP $[(0/90)_2]_S$. The electric conductivity in the fiber, in the transverse, and in the thickness directions that were required to be

analyzed were measured using an actual CFRP specimen (T800S/3900-2B, P2352W-19: Toray Industries Inc., Tokyo, Japan). The specimen stacking sequence was the same as that of the analysis model. Toray T800S/3900-2B is a toughened CFRP with resin-rich interlaminae (the thickness of each ply is 0.19 mm). Because the electric conductivity in the fiber direction is proportional to the fiber volume fraction, CFRP ply that is several times thicker than the diameter of the carbon fiber can be regarded as an electrically homogeneous material in the fiber direction. Although the electric conductivity in the transverse direction depends on the contact among the carbon fibers, the CFRP ply can also be regarded as electrically homogeneous in the transverse direction. This is because many fibers have good contact with each other in the fiber bundles. The CFRP ply is, however, heterogeneous in the thickness direction because the electric conductivity in the thickness direction also depends on fiber contact, and the dimension of the resin-rich layer is not negligibly small compared with the ply thickness.

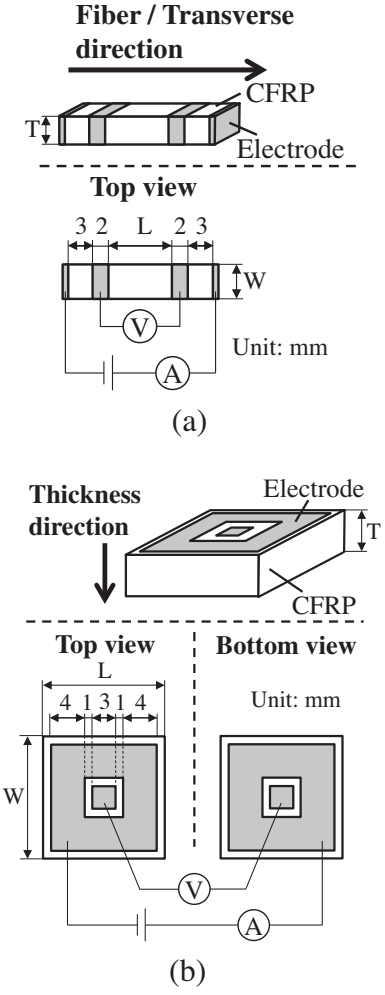

Figure 6. Schematic representation of the specimen for measuring electric conductance by four-probe methods, (a) fiber and transverse direction, and (b) thickness direction.

Table 1. Size of the specimens and measured electric conductance (T800S/3900-2B).

	Length, L [mm]	Width, W [mm]	Thickness, T [mm]	Electric conductance [S/m]
Fiber direction #1	10.93	3.57	4.97	4.94×10^{4}
Fiber direction #2	9.86	3.40	6.46	5.36×10^{4}
Fiber direction #3	9.73	3.37	5.70	4.50×10^{4}
Transverse direction #1	7.34	3.94	6.47	6.55
Transverse direction #2	7.33	3.70	6.42	6.41
Transverse direction #3	7.28	3.83	6.44	6.65
Thickness direction UD#1	14.84	14.72	3.81	3.78×10^{-3}
Thickness direction UD#2	14.83	14.83	3.80	4.00×10^{-3}
Thickness direction UD#3	15.90	14.82	3.79	4.57×10^{-3}
Thickness direction UD#4	15.37	14.64	4.96	3.38×10^{-3}
Thickness direction UD#5	15.45	15.26	4.99	2.44×10^{-3}
Thickness direction CP#1	15.40	16.35	1.48	1.19×10^{-1}
Thickness direction CP#2	15.40	16.35	1.47	4.01×10^{-2}
Thickness direction CP#3	16.21	15.52	1.47	6.06×10^{-2}
Thickness direction CP#4	16.52	15.63	1.45	6.31×10^{-2}
Thickness direction CP#5	15.73	15.67	1.46	8.03×10^{-2}

Figure 6(a) shows a schematic representation of the specimen used for the measurement of the electric conductivity in the fiber and in the transverse direction. Figure 6(b) shows the schematic representation of the specimen used for the measurement of the electric conductivity in the thickness direction. The white area is CFRP, and the gray areas are electrodes made by copper plating. Table 1 shows the dimensions of the specimens. In Table 1, UD means unidirectional CFRP, and CP means cross-ply CFRP. In the present study, all electrodes were made by copper plating to reduce the contact resistance at the electrodes, as described in reference.[12] The four-probe method was adopted to measure the conductivity as shown in Figure 6.

Three specimens were made for measuring the conductivity in the fiber and in the transverse directions, while five specimens were made for the thickness direction measurements because of the larger data scatter than that of the fiber direction or transverse direction. The electric conductivity was measured with an LCR meter (LCR hitester 3522: Hioki E. E. Corporation, Tokyo, Japan) using direct current. The inclination of the relationship between electric current and voltage is used for the measurement.

Figures 7 and 8 show the measurement results. The abscissa is the input current and the ordinate is the measured voltage. The measured results in the fiber direction shown in Figure 7(a) fluctuate in the low current input region. This is because noise has a high influence on the region where the output voltage is very small owing to the small electric resistance in the fiber direction. To prevent experimental error, experimental data above 10 mA were used to obtain the conductivity in the fiber direction for the analysis. For the measurements of conductivity in the transverse direction, the experimental data measured above 0.3 mA were used for the analysis.

Figure 8 shows the measured current–voltage relationship. Figure 8(a) shows the results for the unidirectional CFRP, while Figure 8(b) shows those for the cross-ply CFRP. Although the slopes of the relationships exhibit large scatter, the relationships are almost linear. This means that the resin-rich layer does not play the role of an

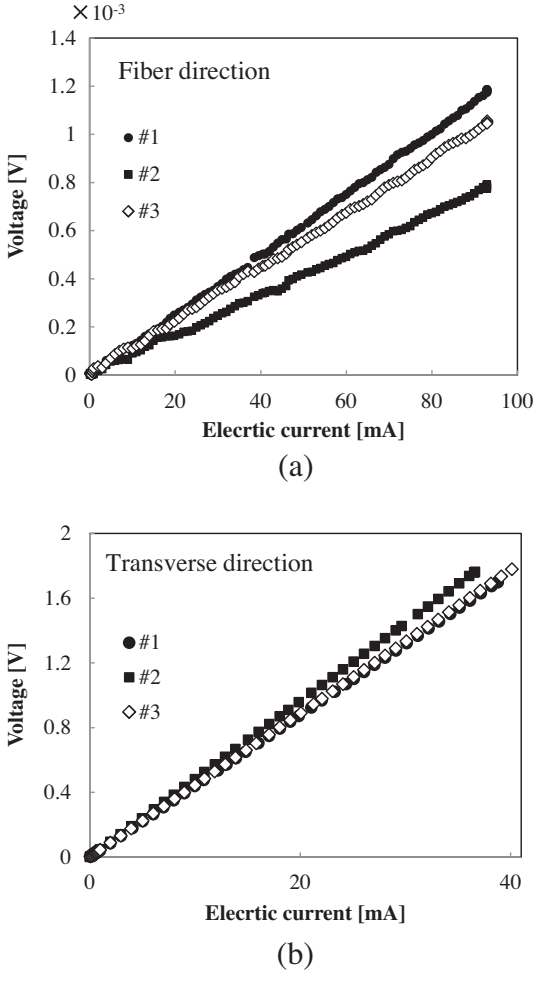

Figure 7. Current–voltage characteristics in (a) fiber direction and (b) transverse direction of CFRP.

insulator. In the present study, our analysis assumes that the electric conductivity in the thickness direction is homogeneous. We use the mean values for the analysis although the data have large scatter.

Table 1 shows the measured conductivity of each specimen. The measured values have large scatter, especially in the case of the cross-ply CFRP laminates. As shown in the reference [13], the conductivity in the thickness direction severely depends on local fiber volume fraction that is caused by fabrication process. This indicates that the conductivity in the thickness direction may depend on the fabrication process. Table 2 shows the values of the electric conductivity used for the analysis. As shown in Table 2, the electrical conductivity is very strongly orthotropic. The electric conductivity in the thickness direction of the unidirectional CFRP is approximately 20 times larger than that of the cross-ply CFRP.

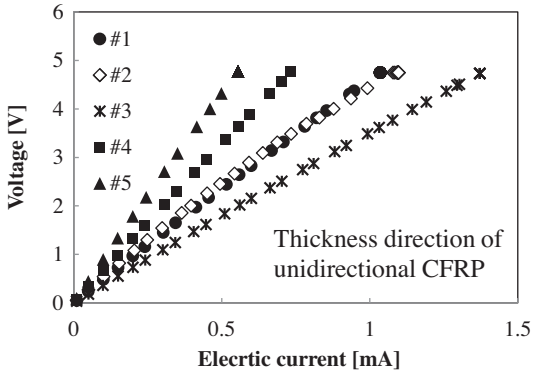

(a)

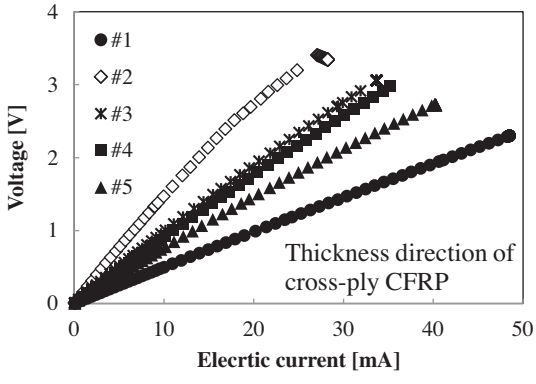

(b)

Figure 8. Current–voltage characteristics in thickness direction, (a) unidirectional CFRP, and (b) cross-ply CFRP.

3. Experimental approach

3.1. Examination of experimental method

In the present study, the electric current that flowed in each ply of the laminated specimen illustrated in Figure 9 was experimentally measured. To measure the electric current in each ply, two CFRP laminates with electrically delaminated plies at their edges were fabricated by inserting polytetrafluoroethylene film at the interlamina, and the specimens were connected through corresponding plies by lead wires as shown in Figure 10. The current flowing in each ply converged on the center lead wire. Therefore, the amount of current flowing in each ply could be measured by measurement of the current flowing in each lead wire.

Table 2. Electric conductance of CFRP laminates (T800S/3900-2B).

		Thickness direction	
Fiber direction	Transverse direction	Unidirectional CFRP	Cross ply CFRP
4.93×10^{4} [S/m]	6.54 [S/m]	3.63×10^{-3} [S/m]	7.25×10^{-2} [S/m]

The effect of making the electrically delaminated area and the effect of using lead wires to connect the two specimens were negligible. In the specimens, the delamination and the lead wires were electrically insulating with respect to the thickness direction. These insulators were placed at the center between the current input source and the output sink. The electric current flowing in these central parts between the two specimens had only a longitudinal component, and the current in the thickness direction was almost zero because of the symmetric configuration. Appropriate design of the dimension of the lead wire and delamination length, however, is required to minimize the disturbance of the electric current caused by the lead wire and the delaminations. Otherwise, the analysis may have given different electric current from the experiments.

To evaluate the effect of the delaminations and lead wires, the amount of electric current in the thickness direction that passed through the interlamina between the first ply and the second ply ($z = 0.19$ mm) and the current passing through that between second ply and third ply ($z = 0.38$ mm) is calculated using the analysis method using Equations (1) and (6). Figure 11 shows the analytical results of i_z normalized by the representative x-directional current density i_{xa}, at a depth of $z = 0.19$ mm and $z = 0.38$ mm: i_{xa} is the mean value of i_x from $x = -220$ mm to $x = 0$; the distance corresponds to the length from the electrode to the center of the specimen. The abscissa is the x-coordinate [mm] and the ordinate is the current density in z-direction i_z normalized by i_{xa}. The solid curve represents the distribution at the depth of $z = 0.19$ mm, and the broken curve represents the distribution at the depth of $z = 0.38$ mm. Because the scale of the ordinate is 10^{-6}, it is clear that the electric current in the thickness direction is negligibly small compared with i_{xa} around the center ($x = 0$).

To calculate the total amount of electric current passing through the interlaminae between plies in the section from $x = -70$ mm to $x = 0$ mm, the electric current in the thickness direction is integrated with respect to the x-direction at the interlamina between the first and the second ply and the x-direction at the interlamina between the second and the third. The results are shown in Table 3. The total electric current passing through the interlamina between the first and the second ply ($z = 0.19$ mm) is only 0.2% of the input current. The delamination of these sections had negligible effect on the current distribution of the CFRP laminates. Therefore, delamination and connection of the lead wires are acceptable at the section from $x = -70$ mm to $x = 0$ mm.

The length of the lead wire was chosen to be 40 mm, and the delamination length for each laminate was 50 mm. Electrodes were mounted at the edge of the laminates with the lead wire using an electrical copper plating method as described in reference [12]. For unidirectional CFRP, two kinds of laminates were fabricated: a specimen with delaminations placed at every interlamina, and a specimen in which the two plies were coupled and the delamination was placed every other interlamina. For cross-ply CFRP,

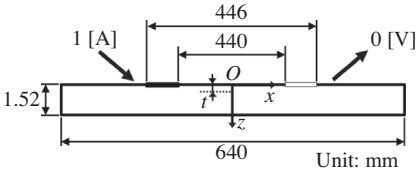

Figure 9. Electric current analysis model of a finite CFRP plate with an electric current input and output lines.

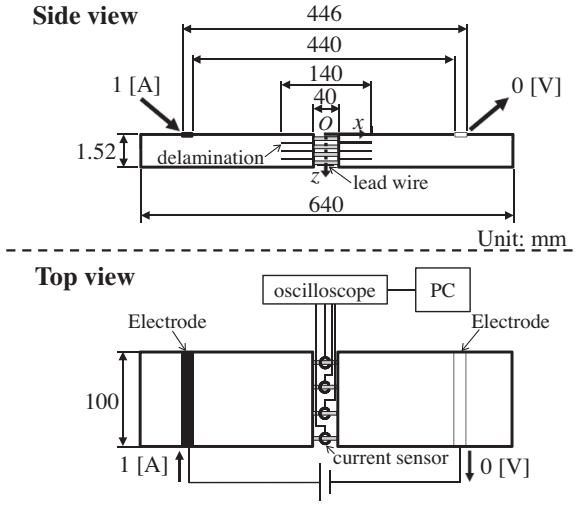

Figure 10. Schematic representation of the experimental model for electric current of CFRP laminates.

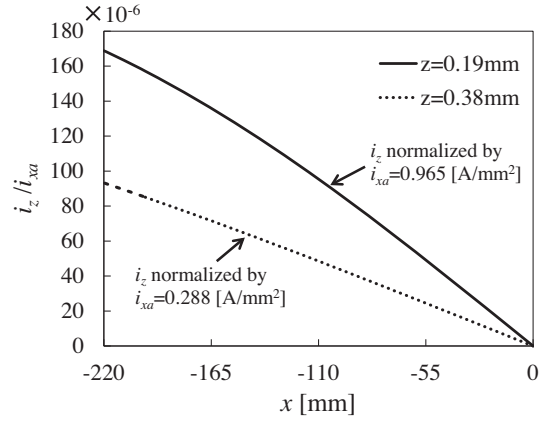

Figure 11. i_z normalized by i_{xa} at $z = 0.19$ [mm] and $z = 0.38$ [mm].

Table 3. Electric current which flows through the analysis target area from $x = -70$ [mm] to $x = 0$.

Position	$z = 0.19$ mm	$z = 0.38$ mm
Electric current [mA]	2.15	0.32

only one specimen was fabricated, one in which the two plies were coupled and the delaminations were placed at every other interlamina, because it is difficult to keep separated 90°-plies unbroken. In the case where the two plies were coupled, the electrodes at the edge of these two plies had identical potential because of the copper plating. This, however, had a small effect on the current distribution because no electric

potential difference in the thickness direction existed at the center of the specimen, as shown in Figure 11.

Figure 10 shows the top view schematic representation of the specimen. The specimen length is 640 mm, and the specimen width is 100 mm. The specimen thickness without delaminations is 1.52 mm. Because the conductivity of copper is 10^3 times higher than that of CFRP in the fiber direction, the copper electrodes on the specimen top surface were treated as areas with identical electric potential. To measure the electric current, non-contact current sensors using the Hall effect (MCS-SD2537: GRID Inc., HDCC-30 mA-D1, HDCC-3 mA-D1: Hohkohsya, Tokyo, Japan) were attached to the lead wires. Current sensors based on the Hall effect do not affect the current

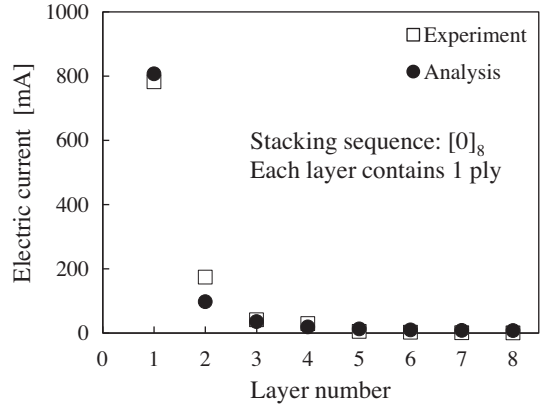

Figure 12. Comparison of experiment and analysis results of electric current flowing at each separated ply which consists of one ply of unidirectional CFRP $[0]_8$.

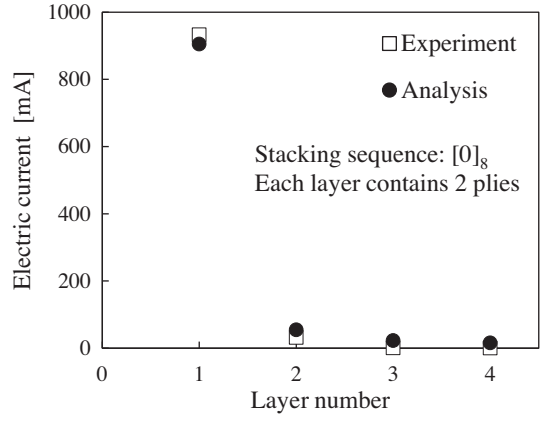

Figure 13. Comparison of experiment and analysis results of electric current flowing at each separated ply which consists of two plies of unidirectional CFRP $[0]_8$.

distribution. The current sensors were connected to an oscilloscope (Picoscope4424: Pico Technology, Tokyo, Japan), and DC source power supply equipment (PW18-1.3AT: Kenwood, Tokyo, Japan) was used to input 1.0 A current.

3.2. *Comparison of the results*

The experimental results obtained for unidirectional CFRP are shown in Figures 12 and 13, and those for cross-ply CFRP are shown in Figure 14. Figure 12 shows the results for the specimen in which delaminations were placed at every interlamina. Figures 13 and 14 show results for the specimens in which the delaminations were placed at every

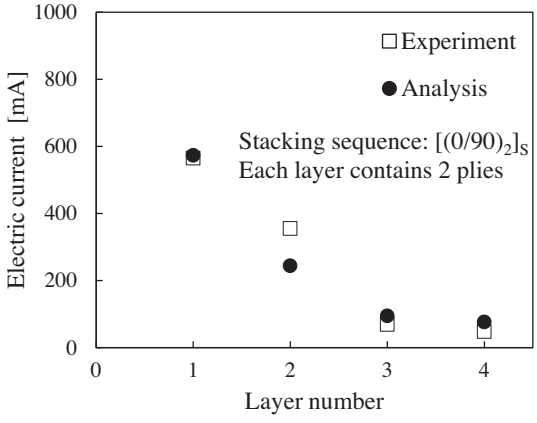

Figure 14. Comparison of experiment and analysis results of electric current flowing at each separated ply which consists of two plies of cross-ply CFRP $[(0/90)_2]_s$.

Table 4. Comparison of experiment and analysis results of electric current flowing at each separated layer.

	Stacking sequence	Layer number	Experiment [mA]	Analysis [mA]
1	$[0]_8$	1	782.11	806.93
		2	174.00	97.45
		3	41.31	35.29
		4	29.22	19.06
		5	5.07	12.63
		6	2.23	9.58
		7	0.50	8.06
		8	0.37	7.41
2	$[0]_8$	1	932.12	904.38
		2	31.47	54.35
		3	0.53	22.21
		4	0.04	15.46
3	$[0/90]_{2S}$	1	564.63	573.26
		2	355.16	243.94
		3	69.39	94.80
		4	47.72	76.54

other interlamina. The abscissa represents the separated layer number. For example, layer number 1 corresponds to the layer including the top surface ply. The ordinate represents the electric current flowing in each layer. In these figures, 'Experiment' means the experimental data and 'Analysis' means the analysis data. The actual values of the current in each layer are listed in Table 4.

Figure 12 shows that the experimental results agree very well with the analysis results. As mentioned in Section 2.3, the experimental results exhibit scatter owing to the large variation in conductance in the thickness direction. From these results, the design of the specimen to minimize the effect of the placement of the delaminations in the middle area of electric current flow is confirmed to be acceptable.

Figure 13 shows that the experimental results agree very well with the analysis results, even for the specimen in which delaminations were placed at every other interlamina. This indicates that the placement of delaminations at every other ply had only a very small effect on the electric current distribution.

The experimental results shown in Figure 14 for the cross-ply CFRP laminates also agree very well with the analysis results. This confirms that the present analytical method using the equivalent electric conductance is effective for electric current analysis of actual CFRP cross-ply laminates.

The above excellent agreements show that the present analytical method is experimentally proven to be effective for actual CFRP laminates that have electrical heterogeneity in the thickness direction. Thus, the present study experimentally verifies the assumption that CFRP laminates are electrically homogeneous orthotropic materials.

4. Conclusions

The present study has experimentally verified the effectiveness of an analytical method that assumes CFRP laminates are homogeneous orthotropic materials for analysis of actual CFRP laminates, even if the CFRP laminates have electrical heterogeneity in the thickness direction. The analysis method was improved to match the actual specimen conditions, and a specimen configuration suitable for measuring the electric current in each ply was designed. Using non-contact current sensors, the electric current in unidirectional CFRP and cross-ply CFRP laminates was measured, and the experimental results were compared with the analysis results. The results obtained are as follows.

(1) Improved electric potential for the finite-length current source and sink has been obtained.
(2) To measure the current in each ply, a newly designed specimen and experimental method that does not disturb the current distribution has been proposed.
(3) The analysis results agree very well with the experimental results. Although the actual toughened CFRP laminates have electrical heterogeneity in the thickness direction, they can be treated as electrically homogeneous orthotropic materials.

Nomenclature

Symbol	Explanation
x	Longitudinal direction
z	Thickness direction
i_x	Electric current density in x-direction
i_z	Electric current density in z-direction
σ_x	Electric conductance in x-direction
σ_z	Electric conductance in z-direction
ϕ	Electric potential
I	Total electric current input
A	Distance of a source or a sink from the center of the specimen
t_1	Distance from inner part of an electrode from the center of the specimen
t_2	Distance from outer part of an electrode from the center of the specimen
ϕ'	Electric potential of the point source of the line
δ_t	Percentage of electric current flowing in the finite plate to input current
T	Thickness of a ply
N	Number of mirror images
$\overline{\sigma_x}$	Equivalent electric conductance in the x-direction
z_k	Depth from the surface

Disclosure statement

No potential conflict of interest was reported by the authors.

References

[1] Gagné M, Therriault D. Lightning strike protection of composites. Prog. Aerosp. Sci. 2014;64:1–16.
[2] Hirano Y, Katsumata S, Iwahori Y, et al. Artificial lightning testing on graphite/epoxy composite laminate. Composites Part A. 2010;41:1461–1470.
[3] Feraboli P, Miller M. Damage resistance and tolerance of carbon/epoxy composite coupons subjected to simulated lightning strike. Composites Part A. 2009;40:954–967.
[4] Ogasawara T, Hirano Y, Yoshimura A. Coupled thermal-electrical analysis for carbon fiber/epoxy composites exposed to simulated lightning current. Composites Part A. 2010;41:973–981.
[5] Abdelal G, Murphy A. Nonlinear numerical modelling of lightning strike effect on composite panels with temperature dependent material properties. Compos. Struct. 2014;109:268–278.
[6] Taketa I, Okabe T, Kitano A. Strength improvement in unidirectional arrayed chopped strands with interlaminar toughening. Composites Part A. 2009;40:1174–1178.
[7] Todoroki A. Electric current analysis of CFRP using perfect fluid potential flow. Trans. Jpn Soc. Aeronautic. Space Sci. 2012;55:183–190.
[8] Todoroki A. New analytical method for electric current and multiple delamination cracks for thin CFRP cross-ply laminates using equivalent electric conductance. Adv. Compos. Mater. Forthcoming.
[9] Katz J, Plotkin A. Low-speed aerodynamics. 2nd ed. New York (NY): Cambridge University Press; 2011.
[10] Todoroki A, Arai M. Simple electric-voltage-change-analysis method for delamination of thin CFRP laminates using anisotropic electric potential function. Adv. Compos. Mater. 2014;23:261–273.
[11] Todoroki A. Electric current analysis for thick laminated CFRP composites. Trans. Jpn Soc. Aeronautic. Space Sci. 2012;55:237–243.

[12] Todoroki A, Samejima Y, Hirano Y, et al. Mechanism of electrical resistance change of a thin CFRP beam after delamination cracking. J. Solid Mech. Mater. Eng. 2010;4:1–11.
[13] Todoroki A, Tanaka M, Shimamura Y. Measurement of orthotropic electric conductance of CFRP laminates and analysis of the effect on delamination monitoring with electric resistance change method. Compos. Sci. Technol. 2002;62:619–628.